논문 96-5-5-01

# Characterization of EFG Si Solar Cells

S. H. Park (朴世薰)*


## Abstract

Solar cells made of the edge-defined film-fed growth Si are characterized using current-voltage, surface photovoltage, electron beam induced curent, electron microprobe, scanning electron microscopy, and electron backscattering. The weak temperature dependence of the I-V curves in the EFG solar cells is due to a voltage variable shunt resistance giving higher diode ideality factors than the ideal one. The voltage variable shunt resistance is modeled by a modified recombination mechanism which includes carrier tunneling to distributed impurity energy states in the band gap within the space-charge region. The junction integrity and the substrate quality are characterized simultaneously by combining I-V and surface photovoltage (SPV) measurements. The diode ideality factors and the surface photovoltages characterize the junction integrity while the SPV diffusion lengths characterizes the substrate quality. Most of the measured samples show the voltage variable shunt resistance although how serious it is depends on the solar cell efficiency. The voltage variable shunt resistance is understood as one of the most important factors of the degradation of EFG solar cells.

## 요 약

EFG Si 태양전지를 전류-전압, 표면광전압, 전자빔유도전류, 전자미세프로브, 전자역산란의 여러 가지 기술을 이용하여 분석하였다. 전류-전압 그래프를 여러 온도에서 측정한 결과 EFG-Si 태양전지는 전압에 따라 변하는 shunt저항을 가진 것이 밝혀졌다. 이러한 shunt저항은 precipitate와 grain boundary에 의해 생긴 것으로 공간전하영역 내의 불순물 에너지 준위로 tunneling에 의해 이동한 캐리어의 재결합으로 일어난 결과이다. 전류-전압과 표면광전압 기술을 결합하면 태양전지의 pn접합과 기판 (substrate)을 동시에 분석할 수 있다. Diode ideality factor와 표면광전압은 pn접합의 특성을, 소수캐리어 확산거리는 substrate특성을 표시한다. EFG 태양전지를 분석한 결과, 전압에 따라 변하는 shunt 저항은 효율에 따라 정도의 차이는 있지만 모든 시편에서 발견되며, 태양전지의 성능을 저하시키는 중요한 원인 중의 하나가 된다.


## I. Introduction

A solar cell performance can be characterized by three main parameters: the open circuit voltage $V_{oc}$, the short circuit current $I_{sc}$, and the fill factor. These three parameters are dependent on both the junction integrity and the substrate quailty. The integrity of the pn junction is characterized by the diode ideality factor and the shunt resistance. The diode ideality factor and the shunt resistance may depend on each other, with lower shunt resistance giving higher diode ideality factor. The substrate quality is determined by the minority carrier recombination lifetime or the minority carrier diffusion length and the series

* School of Electronic and Information Industrial Engineering Andong National University.
Song Chun Dong 388 Andong, Korea
<접수일자 : 1996년 5월 31일>

resistance mainly due to the contact resistance and the bulk resistance of the p and n quasi-neutral regions.

The edge-defined film-fed growth (EFG) Si solar cell is for low-cost terretrial uses. To compete with the fossile fuels like oil and coal, EFG Si film is grown using the low grade Si and cost effective growth method, called the edge-defined film-fed growth technique. EFG films are pulled through a carbon die from Si melt. The grown film have the length of 10 m, the width of 10 cm, and the thickness of 500 $\mu$m. For solar cells, the films are cut into substrates of 5x10 $cm^2$ by laser. There is no wafering process required for Si wafers for integrated circuits saving cost. The grown film is a polycrystalline with crystalline defects such as the grain boundaries and precipitates, which degrade the junction and substrate properties[1]. The solar cells are fabricated using a cheap process making simple pn junctions at the front sides of the solar cells. The EFG solar cells have continuously distributed energy levels over a wide energy range, as determined by the deep-level transient spectroscopy (DLTS)[2]. The EFG solar cell is a rectangular of 5x10 $cm^2$ with the substrate B doping of about $1x10^{16}$ $cm^{-3}$. Typical values of the solar cell parameters are that $J_{sc}$=30 mA/$cm^2$, $V_{oc}$=0.55 V, fill factor=0.7, efficiency=12%, series resistance=5 $\Omega$, and shunt resistance=600 k$\Omega$.

In this study, EFG solar cells are characterized by several techniques, including forward I-V curves, surface photovoltage (SPV), DLTS, scanning electron microscopy (SEM), electron beam induced current (EBIC), electron backscattering, and energy-dispersive spectrometry (EDS). The forward I-V curve is the simplest technique and provides the most information on the pn junction quality. The diode ideality factor, series resistance, and shunt resistance are obtained from dark forward I-V curves, while the short circuit current, open circuit voltage, and fill factor are obtained from illuminated forward I-V curves. The dark forward I-V curve reveals the source of the leakage current when temperature is varied. Surface photovoltage is particularly attractive for diffusion length measurements because the physical phenomenon used in the measurement is the same as that leading to power production in the solar cell. SPV also measures the surface photovoltage $V_{SPV}$-the open circuit voltage of the diode.

Mesa diodes were prepared for the measurements of I-V, SPV, and EBIC. The mesa diodes, with diameters ranging from 1 mm to 2 mm, are convenient devices to observe the effect of specific defects or impurities on the electrical parameters such as the diffusion length $L_n$, the open circuit voltage $V_{oc}$, and the diode ideality factor n.

## II. Characterization of EFG Si Solar Cells

### 1. Theoretical Dark I-V Characteristics of Normal Diodes

Dark I-V characteristics contain important information on the integrity of pn junctions. The high impurity concentration and the high density of crystalline defects in low-cost charge materials and the cost-efficient growth processes often lead to poor junctions. It is known that n=1 for recombination current in the quasi-neutral regions and n=2 for recombination current in the space-charge region. Normal diodes, therefore, usually have ideality factors between 1 and 2. However, the pn junctions of low cost solar cells such as EFG Si and CAST Si sometimes have higher values of n. Grain boundaries decorated with metal impurities provide a leakage path across the junction. The deep level defects continuously distributed in the band gap along the grain boundaries also give rise to leakage current paths, causing decreased shunt resistance.

The diode dark current J is

$$J= \frac{q D_n n_i^2}{N_a L_n} \exp\left(\frac{q(V-IR_s)}{kT}\right) + \frac{qWn_i}{2\tau_{scr}} \frac{q(V-IR_s)}{2kT} + \frac{(V-IR_s)}{AR_{sh}} \quad (1)$$

where $D_n$ is the electron diffusion coefficient, $n_i$ the intrinsic carrier density, $N_a$ the lightly doped p region doping density, $L_n$ the electron diffusion length, $R_s$ the series resistance, W the space-charge region width, $\tau_{scr}$ the lifetime in the space-charge region, A the device area, and $R_{sh}$ the shunt resistance. The first term on right side of Eq. (1) accounts for the recombination current in the quasi-neutral substrate and the second term accounts for the recombination current in the space-charge region. The third term expresses the current through the shunt resistance $R_{sh}$. Recombination in the quasi-neutral $n^+$-emitter has been neglected because it is small compared to the substrate current.

The theoretical dark forward current vs. voltage is calculated using Eq. (1) and shown in Fig 1. with temperature as a parameter. For calculations used values are $R_s$ = 1 Ω, $\tau_{scr}$ = 1 μs, and $R_{sh}$=1 MΩ. Fig 1. shows the current through the shunt resistance to dominate the recombination current in the space-charge region for all of the temperatures.

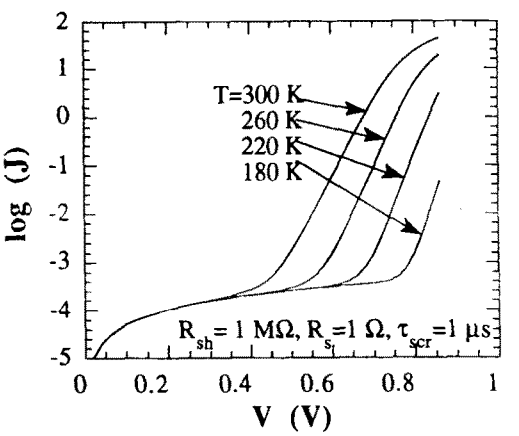


Fig. 1. Theoretical current density vs. voltage as a function of temperature.

## 2. Dark I-V and SPV characteristics of EFG Solar Cells

Dark forward I-V and SPV measurements were made on the mesa diodes selected from both Cr-doped solar cell 4706-3 and undoped, high efficiency solar cell 1921-1. The output powers of the Cr-doped and high-efficiency cells are 11 mW/cm$^2$ and 13 mW/cm$^2$ with the incident energy of 100 mW/cm$^2$, respectively. The dark forward I-V curves measured as a function of temperature reveal important information on the junction integrity and the tunneling leakage paths of the junction. The diode ideality factor is calculated from the dark forward I-V curves using

$$n = \frac{1}{kT\frac{d\ln J}{dV}} \quad (2)$$

Three samples are selected from the Cr-doped cell and two samples from the high-efficiency cell. The three samples from the Cr-doped cell are located within the area of a 2 cm$^2$ rash-free region. 'Rash' is a second phase formation caused by an effective unity segregation coefficient due to the die shape and the high growth rate of EFG Si[1,3]. The J-V and n-V curves measured at room temperature are shown along with $V_{spv}$ and $L_n$ data in Fig. 2(a) and (b) respectively. Sample 4706-3 (2.7) shows high values of surface photovoltage and diffusion length and samples 4706-3 (4.6) and (4.3) have low values of $L_n$ and $V_{spv}$. For the latter two samples of low $L_n$, the $V_{spv}$ of sample 4706-3 (4.6) is much higher than that of sample 4706-3 (4.3) implying that $L_n$ and $V_{spv}$ characterize different parts of the cell.

Samples 4706-3 (4.3) and (4.6) have higher current at low voltage than sample 4706-3 (2.7). The first two appear to have additional current paths other than space-charge recombination at low voltages assuming 4706-3 (2.7) to be close to ideal. The additional current paths degrade the

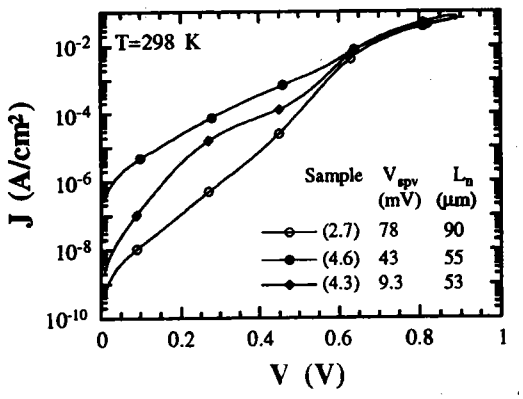


(a)

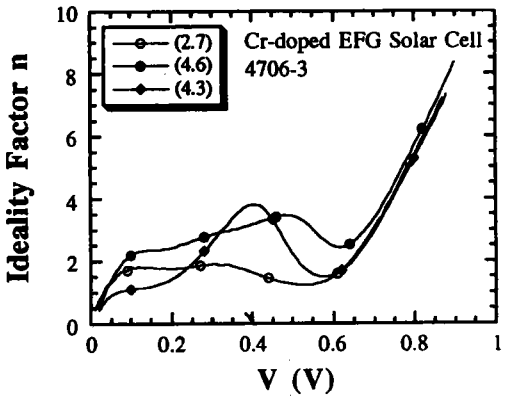


(b)

Fig. 2. (a) Dark J-V and
(b) n-V characteristics of Cr-doped EFG solar cell at 298 K.

junction integrity resulting in the low open circuit voltage and low short circuit current. This additional current at low voltage is due to the junction shunt resistance. However, the shunt resistance is not a simple passive component but is a voltage variable. The diode ideality factors are shown in Fig. 2(b). Samples 4706-3 (4.3) and (4.6) have n values up to 4 at room temperature at low voltage, whereas for sample 4706-3 (2.7) n=1-2. By combing the $V_{SPV}$ with the diode ideality factors, it is found that the lower n a cell has, the higher is its $V_{SPV}$.

Although I-V curves reveal the existence of problems with junction quality, it is difficult to tell the source of the problems. By varying the measurement temperature, the I-V curves reveal important information on the junction quality. I-V curves of Cr-doped EFG solar cells 4706-3 (4.3) and (2.7), measured at various temperatures, are shown in Fig. 3(a) and Fig. 4(a) respectively. The temperature dependent current exhibits behavior not found for room-temperature I-V curves. Comparison of the temperature dependence of the measured I-V curves with that of the calculated J-V of Fig. 1 confirms the abnormality of Fig. 3(a) and 4 (a). The diode ideality factors of samples, 4706-3 (4.3) and (2.7), are shown with temperature as a parameter in Figs. 3(b) and 4(b).

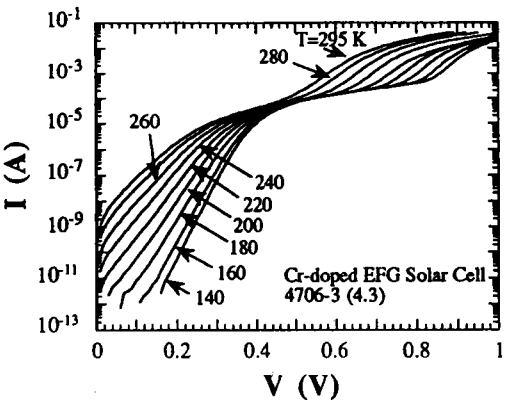


(a)

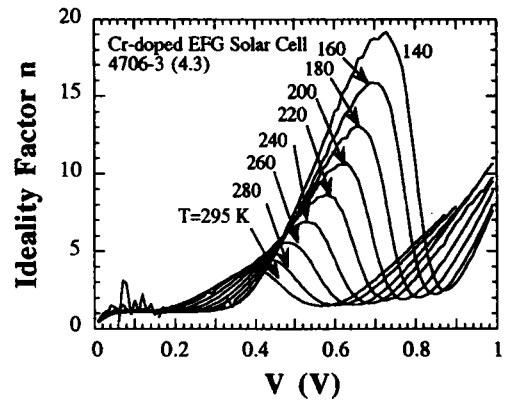


(b)

Fig. 3. (a) I-V and (b) n-V characteristics of Cr-doped EFG solar cell 4706-3 (4.3) as a function of temperature.

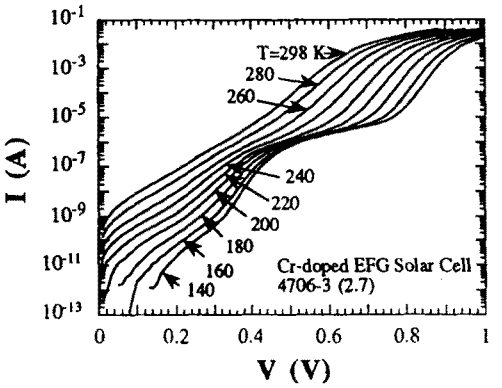


(a)

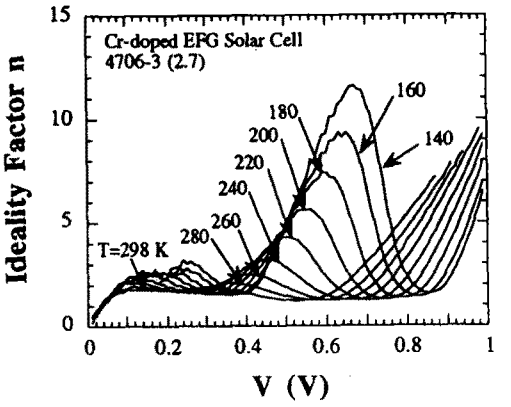


(b)

Fig. 4. (a) I-V and (b) n-V characteristics of Cr-doped EFG solar cell 4706-3 (2.7) as a function of temperature.

Sample 4706-3 (4.3) shows weak temperature dependent I-V curves as shown in Fig. 3(a). In Fig. 3(b), the diode ideality factor shows a maximum followed by a deep minimum. Beyond that, n increases again as the series resistance becomes dominant at high level injection. The dip in the n-V plot is attributed to recombination current in the quasi-neutral regions. The plot of n-V shifts as temperature is reduced. At the lower temperatures, fewer carriers are available for current. To compensate for the reduced carriers at the lower temperatures, a higher voltage is necessary shifting the I-V and n-V curves toward higher voltages. In sample 4706-3 (4.3), n reaches 4 even at room temperature. The increase of $n_{max}$ with decreasing temperature is due to Shockly-Read-Hall (SRH) recombination current becoming less important at low temperatures.

Sample 4706-3 (2.7) is closest to the ideal SRH recombination current in terms of the diode ideality factor at room temperature. I-V and n-V curves with temperature variation of sample 4706-3 (4.3), however, are quite different from those of sample 4706-3 (2.7) as shown in Figs. 3 and 4 respectively. The weak temperature dependence of the current of sample 4706-3 (2.7) appears at T=220 K and below while that of sample 4706-3 (4.3) appears even at room temperature. In addition, $n_{max}$ of sample 4706-3 (2.7) is 11 while $n_{max}$ of sample 4706-3 (4.3) reaches 19 at T=140 K. The temperature dependence of I-V characteristics reveals that the lower temperature dependence of I-V and higher $n_{max}$ of samples 4706-3 (4.3) is responsible for the low value of $V_{SPV}$. Most of Cr doped samples show a similar temperature dependent current. This implies that the Cr-doped solar cell has poor junction integrity due to Cr-related precipitates in the space-charge region regardless of the substrate quality. The lower temperature dependence of the I-V curves occurs only in a small region around V=0.5 V. As shown in Fig. 1 the calculated J-V curves using the model with a fixed shunt resistance have a weak temperature dependence over a wide range of low voltages. The weak temperature dependence of the I-V curves is believed to be the result of a voltage variable shunt resistance.

$V_{SPV}$ of sample 4706-3 (2.7) is very high compared to the other two samples 4706-3 (4.3) and (4.6) although I-V curves of sample 4706-3 (2.7) also exhibit a temperature insensitive portion even at relatively low temperature. This is because $V_{SPV}$ depends not only on n but also on the $L_n$. Carriers of high diffusion length have

higher probability of being collected by the electric field in the space-charge region to generate higher $V_{SPV}$ than those of low diffusion length. In the case of sample 4706-3 (2.7), high diffusion length of carrier contributes more to $V_{SPV}$ than the voltage variable shunt resistance reduces $V_{SPV}$.

Dark forward I-V curves of high-efficiency EFG solar cells were also measured on two samples. The two samples are selected for discussion since they have quite different $V_{SPV}$ values in spite of similar high diffusion lengths. Sample 1921-1 (6.6) has much higher $V_{SPV}$ than sample 1921-1 (5.2). The open circuit voltage is mainly determined by the electrical properties of the junction while the diffusion length is determined by the electrical properties of the substrate. The open circuit voltage and diffusion length are, however, not completely independent of each other. Fig 5. shows the J-V curves of two samples at room temperature. The current of sample with low $V_{SPV}$ is higher than that of the sample with high Vspv at the low voltage range implying the additional current paths of the high $V_{SPV}$ sample over the low $V_{SPV}$ sample.

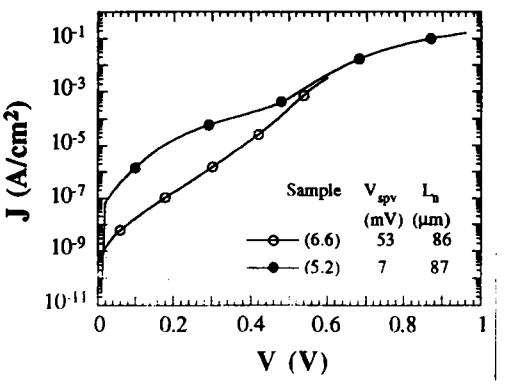


Fig. 5. Current density-voltage characteristics of high-efficiency EFG solar cell 1921-1 at room temperature.

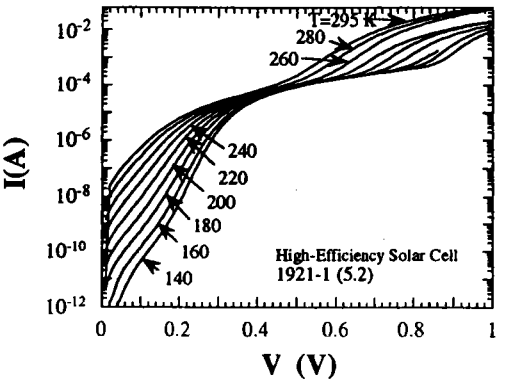


(a)

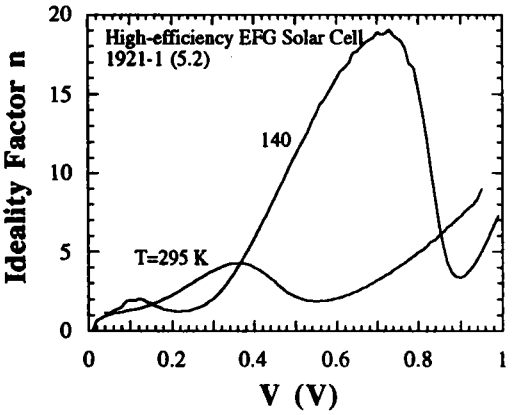


(b)

Fig. 6. (a) I-V and (b) n-V characteristics of a high-efficiency EFG solar cell 1921-1 (6.6) as a function of temperature.

Figs 6 and 7 compare both I-V and n-V curves of two samples showing quite different temperature behavior. Figs. 6(a) and (b) show the I-V curves and n-V curves for sample 1921-1 (6.6) respectively. This sample shows the normal temperature dependence of current and diode ideality factor. The diode ideality factor at room temperature is close to the theoretical values between 1 and 2. Even at T=140 K, there is no peak in the n values. The value of n at T=140 K is below 3. On the other hand, Fig. 7 of sample 1921-1 (5.2) shows abnormal I-V and n-V curves. The sample of low $V_{SPV}$ has very weak

temperature dependence of current and high n value for the voltage range as found in Cr-doped samples. This confirms that low $V_{SPV}$ is closely related to the weak temperature dependence of I-V curves. As a voltage variable shunt resistance due to deep level impurities is common in EFG solar cells, it is necessary to understand how such a voltage variable shunt resistance forms. A qualitative model of the voltage variable shunt resistance is suggested below.

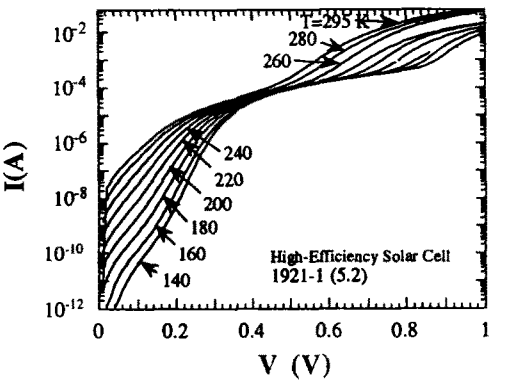


(a)

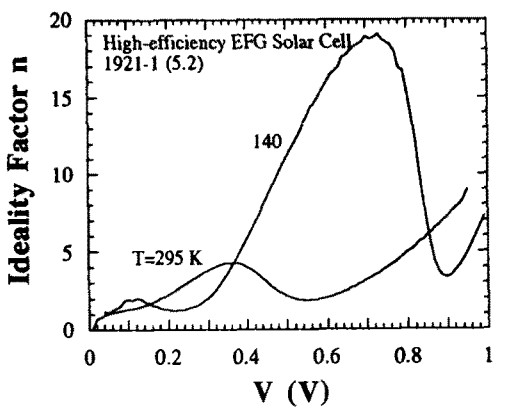


(b)

Fig. 7. (a) I-V and (b) n-V characteristics of a high-efficiency EFG solar cell 1921-1 (5.2) as a function of temperature.

## 3. Tunnel Current Characterization of EFG Solar Cell

Temperature-dependent current-voltage measurements show the existence of a voltage variable shunt resistance of EFG solar cells, degrading solar cell performance. Hence, main concern is about what causes the voltage variable shunt resistance of EFG solar cells. The additional current component through the voltage variable shunt resistance is not explained by the conventional Sah-Noyce-Shockley (SNS) model[4]. Instead, a new recombination model is needed to include the high diode ideality factor and the weak temperature dependence of the I-V curves. The diode ideality factor increases with decreasing temperature and the activation energy is extremely low at a voltage where the I-V curves show very weak temperature dependence. These properties are consistent with a tunneling current[5,6].

A model is proposed to explain the additional current through the voltage variable shunt resistance by a tunnel current, composed of two steps: tunneling and recombination of the carriers. As the first step, tunneling of carriers is only possible if there are energy states into which the carriers can tunnel from the conduction band or the valence band. The situation is met only in the space-charge region where band bending exists due to the electric field. Energy states in the band gap then are available for tunneling of carriers from the conduction band and/or the valence band to the energy states in the band gap. As the second step, the carriers reaching the energy levels by tunneling recombine with carriers in the space-charge region when the junction is forward biased. This recombination is different from the conventional SNS model because tunneling increases the recombination rate, resulting in an additional current.

A schematic diagram of the tunnel current is dipicted in Fig. 8, showing the energy levels

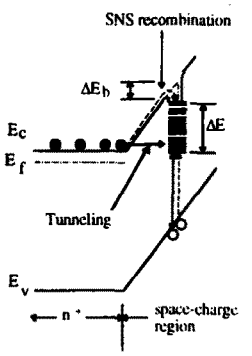


Fig. 8. Schematic band diagram for tunneling and SNS recombination.

distributed over an extended energy interval $\Delta E$. The distribution of energy levels due to grain boundaries and precipitates was confirmed by DLTS measurements of EFG solar cells[2]. Energy states near the $n^+$-region are available for tunneling of electrons from the conduction band. Conventional SNS recombination is represented by the dashed line in the band diagram. Tunneling current is represented by the solid line. Electrons tunneling to states in the band gap recombine with holes giving rise to an increase of current. The tunneling rate is expressed by [6]

$$T \approx \exp(-A)\exp(BV) \tag{3}$$

where A and B are constants depending on the material properties. As a result, the tunnel current is exponentially dependent on the voltage and only weakly dependent temperature. This temperature independence explains the weak temperature dependence of the I-V of EFG solar cells.

In the space-charge region, the diode current density is proportional to the recombination rate of carriers U given by

$$U = n_i\, C_n\, N_T \exp\left(\frac{qV}{2kT}\right) \tag{4}$$

where $C_n$ is the capture rate for electrons and $N_T$ the impurity density. The space-charge region current is exponentially dependent on the voltage in the conventional SNS model resulting in a diode ideality factor of two. In the presence of an electric field, the capture rate $C_n$ can be expressed by

$$C_n = C_o \exp\left(\frac{\Delta E_b}{kT}\right) \tag{5}$$

due to the Frenkel-Pool effect[7]. $C_o$ is the capture rate without electric field, $\Delta E_b$ the barrier lowering due to the electric field. For a Coulombic well, $\Delta E_b$ is given by the expression

$$\Delta E_b = q\sqrt{\frac{qE}{\pi K_s \varepsilon_o}} \tag{6}$$

where $E$ is the electric field. In a pn junction, the electric field decreases with forward bias reducing the value of $\Delta E_b$. The reduced potential barrier lowering decreases the capture rate $C_n$ of Eq. (5) making the pn junction more sensitive to voltage compared to high potential barrier lowering. The current in the space-charge region is no longer expressed by Eq. (4). The exponential term changes from exp(qV/2kT) to exp(V(q/2kT-C)) where C accounts for a decrease of electric field in the space-charge region by the forward bias. As a result, the diode ideality factor n is given now by

$$n = \frac{q/kT}{1/2kT - C} \tag{7}$$

where n increases from 2 to infinity as C goes from 0 to q/2kT.

The distributed energy states of EFG solar cell are investigated with several techniques to determine their identity. Electron beam induced

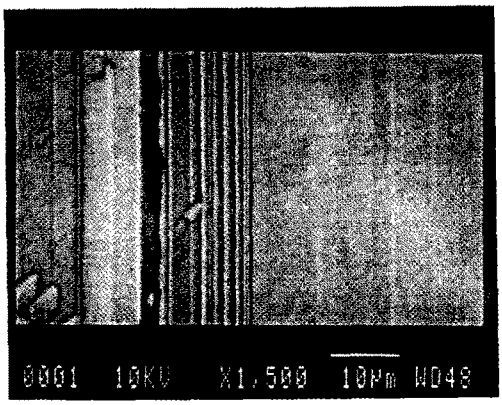


Fig. 9. EBIC image (left) and SEM image (right) of sample 1921-1 (5.2).

current (EBIC) was used to detect recombination centers near the junction (1 $\mu$m below the junction). The recombination centers near the junction appear as black spots when the electron beam-generated electron-hole pairs recombine. On sample 1921-1 (6.6) such recombination centers were rarely detected. On the sample 1921-1 (5.2), on the other hand, there are many black strips on the EBIC image shown in Fig 9. The secondary electron microscopic (SEM) image is compared with the EBIC image in Fig 9. No features are decernible in SEM where the EBIC image shows strong recombination activity. Energy-dispersive spectrometry (EDS) was used to examine the elements in the EBIC spot. Only Si was detected. Electron backscattering was also used to examine the element in the EBIC spot. No elements were found that differed from other areas.

The voltage variable shunt resistance in EFG solar cells is most likely due to a modified recombination including tunneling of carriers to the impurity energy states. These states are believed to be crystalline defects that may be due to intrinsic Si defects or Si precipitates with light atomic number elements, e.g. $SiO_2$, SiC, not detectable with EDS or electron backscattering. Shoulders in dark I-V curves have been attributted by others to surface recombination at the rear surface of high-efficiency solar cells[8]. That mechanism, however, does not apply to our cells, since few carriers reach the rear surface.

### 4. Junction and Substrate Characteristics of EFG Solar Cells

The quality of the junction and the substrate can be simultaneously determined by combining I-V and SPV. In Cr-doped cells, n is found to be reasonably well related to $V_{SPV}$ as shown in Fig 10. The data show that as n increases, $V_{SPV}$ decreases. This trend is also found for other than Cr-doped solar cells and points to the ideality factor as a good indicator of the open circuit voltage. For n $\approx$1-2 surface photovoltages are in the ranges of 50 to 100 mV. These voltages, however, decrease to values in the low mV range for n of 5 or higher. The diffusion length, $L_n$, shows much less correlation with the ideality factor. For example, the mesa diodes on 'rash' areas have shorter diffusion length ($L_n$=65 $\mu$m) than those on 'rash-free' areas ($L_n$=116 $\mu$m), as expected, while n varies little. This is understandable as the substrate diffusion length is determined by the recombination centers in the bulk and by the back surface recombination velocity while the ideality factor is determined by the junction quality.

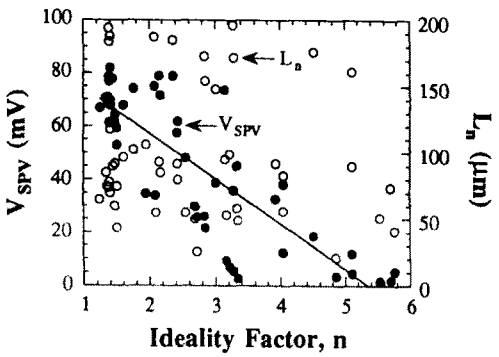


Fig. 10. Surface photovoltage (solid circles) and electron diffusion length (open circles) as a function of diode ideality factor of Cr-doped EFG solar cells.

## III. Conclusions

The voltage variable shunt resistance is one of the major reasons of degradation of EFG solar cells. Current through the voltage variable shunt resistance degrades cell performance reducing the open circuit voltage as well as the short circuit current. The voltage variable shunt resistance is caused by the tunneling aided recombination of carriers in the space-charge region. The tunneling of carriers is possible only when there exit states in the band gap within the space-charge region. Grain boundaries and precipitates generate the deep level impurities to which electrons in the conduction band of $n^+$-region can tunnel. Combining I-V and SPV techniques is useful to estimate the junction integrity and the substrate quality.

## References

[1] J.P. Kalejs, B. Bathy, and C. Dube, "Segregation and impurity effects in silicon", J. Cryst. Growth, vol. 109, pp. 174-180, 1991.

[2] S.H. Park and D.K. Schroder, "Deep-level impurities in edge-defined film-fed growth silicon", J. Appl. Phys., vol. 78, pp. 801-810, 1995.

[3] J.B. Mohr, S.H. Park, S.N. Schauer, D.K. Schroder, and J.P. Kalejs, "Physical and electrical investigation of silicide precipitates in EFG polycrystalline silicon intentionally contaminated with chromium", 21st IEEE Photovoltaic Specialist Conference, Kissimee, FL (IEEE New York), p. 711, 1990.

[4] C.T. Sah, R.N. Noyce, and W. Shockley, "Carrier generation and recombinatin in P-N junctions and P-N junction characteristics", Proc. IRE, vol. 45, pp. 1228-1243, 1957.

[5] E. Hackbarth and D.D-L. Tang, "Inherent and stress-induced leakage in heavily doped silicon junctions", IEEE Trans. Electron Dev., vol. ED-35, pp. 2108-2118, 1988.

[6] J.A. Del Alamo and R.M. Swanson, "Forward-biased tunneling: A limitation to bipolar device scaling", IEEE Electron Dev. Lett., vol. EDL-7, pp. 629-631, 1986.

[7] J, Frenkkel, "On pre-breakdown phenomena in insulators and electronic semiconductors", Phys. Rev., vol 54, pp. 647-648, 1938.

[8] S.J. Robinson, S.R. Wenham, P.P. Altermatt, A.G. Aberle, G. Heiser, and M.A. Green, "Recombination rate saturation mechanisms at oxidized surface of high-efficiency Si solar cells", J. Appl. Phys., vol. 78, pp. 4740-4754, 1995.

## 著 者 紹 介

**박 세 훈**

1957년생, 1980년 경북대학교 전자공학과 졸업(공학사), 1982년 경북대학교 대학원 전자공학과 졸업(공학석사), 1992년 Arizona State University 졸업(공학박사), 1983-1986 현대전자, 1993-1995 한국전자통신연구소, 1995-현재 안동대학교 전자정보산업학부 전임강사, 주관심분야: 반도체 소자, ASIC 설계